New Phytologist

Research

Growth duration is a better predictor of stem increment than carbon supply in a Mediterranean oak forest: implications for assessing forest productivity under climate change

Morine Lempereur[1,2], Nicolas K. Martin-StPaul[3], Claire Damesin[4], Richard Joffre[1], Jean-Marc Ourcival[1], Alain Rocheteau[5] and Serge Rambal[1,6]

[1]Centre d'Ecologie Fonctionnelle et Evolutive CEFE, UMR 5175, CNRS, Université de Montpellier, Université Paul-Valéry Montpellier, EPHE, 1919 Route de Mende, 34293 Montpellier Cedex 5, France; [2]Agence de l'Environnement et de la Maîtrise de l'Energie, 20, Avenue du Grésillé – BP 90406, 49004 Angers Cedex 01, France; [3]Ecologie des Forêts Méditerranéennes, INRA, UR629, F-84914 Avignon, France; [4]Laboratoire Ecologie, Systématique et Evolution (ESE), CNRS AgroParisTech-UMR 8079, Bâtiment 362, Université de Paris-Sud, 91405 Orsay Cedex, France; [5]IRD, CEFE, UMR 5175, 1919 Route de Mende, F-34293 Montpellier Cedex 5, France; [6]Departamento de Biologia, Universidade Federal de Lavras, CP 3037, CEP 37200-000 Lavras, MG, Brazil

Author for correspondence:
Morine Lempereur
Tel: +33 46761392
Email: morine.lempereur@cefe.cnrs.fr

Received: *4 November 2014*
Accepted: *23 February 2015*

New Phytologist (2015)
doi: 10.1111/nph.13400

Key words: carbon partitioning, climate change, drought, extreme event, *Quercus ilex*, tree water relation, vegetation models, water deficit.

Summary

- Understanding whether tree growth is limited by carbon gain (source limitation) or by the direct effect of environmental factors such as water deficit or temperature (sink limitation) is crucial for improving projections of the effects of climate change on forest productivity.
- We studied the relationships between tree basal area (BA) variations, eddy covariance carbon fluxes, predawn water potential (Ψ_{pd}) and temperature at different timescales using an 8-yr dataset and a rainfall exclusion experiment in a *Quercus ilex* Mediterranean coppice.
- At the daily timescale, during periods of low temperature (< 5°C) and high water deficit (< −1.1 MPa), gross primary productivity and net ecosystem productivity remained positive whereas the stem increment was nil. Thus, stem increment appeared limited by drought and temperature rather than by carbon input. Annual growth was accurately predicted by the duration of BA increment during spring (Δt_{t0-t1}). The onset of growth (t_0) was related to winter temperatures and the summer interruption of growth (t_1) to a threshold Ψ_{pd} value of −1.1 MPa.
- We suggest that using environmental drivers (i.e. drought and temperature) to predict stem growth phenology can contribute to an improvement in vegetation models and may change the current projections of Mediterranean forest productivity under climate change scenarios.

Introduction

Forest growth represents a substantial and lasting carbon sink that may mitigate the ongoing rise of atmospheric CO_2 (Bonan, 2008; Pan *et al.*, 2011). In addition, tree growth is often used as a surrogate for tree vitality (Bigler & Bugmann, 2003; Dobbertin, 2005), and an increasing number of studies rely on tree growth to assess whether and which tree species will be able to persist in a changing environment (e.g. Gaucherel *et al.*, 2008; Lévesque *et al.*, 2013). A better understanding of the factors controlling tree growth is therefore crucial to assess the impact of climate change on forests (Babst *et al.*, 2014).

In order to identify the climate determinants of tree growth and to anticipate tree vulnerability under climate change projections, several studies have derived statistical links between tree ring widths and past climate (Gea-Izquierdo *et al.*, 2013; Subedi & Sharma, 2013; Babst *et al.*, 2014). A major advantage of this approach is that it can be applied with relatively little information on the ecology and physiology of the species of interest. However, these empirical models are valid only for the range of environmental conditions used for their parameterization, leading to potentially important uncertainties when extrapolated under climate change scenarios.

Alternative approaches focus on understanding the ecophysiological processes controlling the responses of tree growth to abiotic drivers, including photosynthesis, respiration and biomass partitioning, as well as leaf and growth phenology. With such an ecophysiological basis, process-oriented models are built and used to evaluate the consequences of climate change on forest functioning (e.g. Gaucherel *et al.*, 2008; Keenan *et al.*, 2011; Cheaib *et al.*, 2012). Most of these models consider tree growth to be a constant fraction of the current year gross photosynthesis. This assumption is supported by the positive linear relationship found across biomes between gross photosynthesis and aboveground biomass growth (Litton *et al.*, 2007). However, studies linking different proxies of tree stem growth (e.g. dendrometers, tree

rings or inventory) and eddy covariance (EC) carbon fluxes at finer spatial levels (stand or tree) and temporal resolution (day to year) have yielded contradicting results. Although these differences could arise from the different methodologies used, it may also be that different processes are involved in the growth determinism according to the site and the timescale considered.

Using automatic dendrometers (AD), Zweifel *et al.* (2010) reported very tight associations between stem radial variations and EC fluxes (gross primary productivity, GPP, and net exchange productivity, NEP) at timescales ranging from hours to years in a Norway spruce (*Picea abies*) forest in the Swiss Alps. By contrast, Rocha *et al.* (2006) found no significant correlation between tree ring width and GPP in a mature stand of black spruce forests in Canada, and suggested that the active mobilization of carbon storage may control between-year stem growth variations. This conclusion was reinforced by the study of Richardson *et al.* (2013) who improved the prediction of interannual variations in wood growth in three temperate forests by accounting for the mobilization of carbon storage pools that were several years old. Other studies performed in temperate forests have found intermediate results. For instance, at five sites spanning a wide range of latitudes across Europe, Babst *et al.* (2014) found a significant link between tree ring estimation of annual biomass increment and EC carbon fluxes (GPP and NEP) cumulated over the early growing season (January to June/July). Granier *et al.* (2008) reported robust links between radial growth and spring to early summer carbon fluxes, in a French beech (*Fagus sylvativa*) forest. This suggests an overriding role of the spring period in the stem growth process. Similarly, using manual band dendrometers in another fertile beech forest of Germany, Mund *et al.* (2010) suggested that the length of the growing season, limited by both the effects of spring temperature on cambial reactivation and summer water deficit on growth interruption, exerted a prominent control on growth. These later results are in line with studies that use stem growth phenology as a driver for annual growth (Rossi *et al.*, 2008, 2013). Also, they are consistent with observations that cell division and expansion are more sensitive than photosynthesis to drought and cold stress (Boyer, 1970; Hsiao & Acevedo, 1974; Körner, 2003; Daudet *et al.*, 2005; Muller *et al.*, 2011).

Despite several studies attempting to link stem growth and carbon fluxes, few have explicitly attempted to decipher whether tree growth is more related to carbon availability (i.e. source limitation of growth) or to the direct effect of the environment (i.e. sink limitation of growth) and at which timescale (Daudet *et al.*, 2005). Yet, this question is crucial in the context of climate change because considering tree growth as a source- or a sink-limited process in vegetation models may have a strong impact on forest growth projections (Fatichi *et al.*, 2014). This is particularly important in the Mediterranean region where climate models project a substantial increase in aridity for the end of the century (Gao & Giorgi, 2008; Diffenbaugh & Giorgi, 2012; IPCC, 2014), in line with the increase in water deficit observed in the region over the last decades (Ruffault *et al.*, 2013)

In this study we aimed at understanding whether stem growth is related more to the ecosystem photosynthesis or to environmental constraints (e.g. temperature and water deficit) for a mature Mediterranean evergreen oak *Quercus ilex* coppice by using stem basal area variations (assessed with AD) as a proxy for growth. Our objectives were to assess: the links between stem basal area variations and ecosystem carbon fluxes at different timescale (from daily to yearly); the links between annual stem growth and stem phenology; the links between stem phenology, temperature and water deficit; whether annual growth is more predictable with the drivers of stem growth phenology or to carbon fluxes; and finally the impact of climate change on stem growth at our site.

Materials and Methods

Site description

The study site is located 35 km north-west of Montpellier (southern France), on a flat plateau, in the Puéchabon State Forest (3°35′45″E, 43°44′29″N, 270 m a.s.l.). This forest has been managed as a coppice for centuries and the last clear cut was performed in 1942. Vegetation is largely dominated by a dense overstorey of the evergreen oak *Quercus ilex* L. In 2011, the top canopy height was 5.5 m on average. The stem density of *Q. ilex* evaluated on four plots larger than 100 m^2 was 4703 ($\pm$ 700) stems ha^{-1}. The diameters at breast height (DBH) of *Q. ilex* stems were distributed as follows: 21% of stems were under 6 cm DBH, 44% were between 6 and 8.5 cm and 35% were over 8.5 cm. The climate is Mediterranean with a mean annual precipitation of 903 mm and a mean annual temperature of 13°C (average 1984–2011). The very shallow bed rock imposes a strong constraint on water availability: the volumetric fractional content of stones and rocks averages 0.75 for the top 0–50 cm and 0.90 below. More details on the sites characteristics are available in Rambal *et al.* (2003, 2004, 2014) and in Supporting Information Methods S1.

Experimental design

Stem basal area (BA) variations of individual *Q. ilex* stems were measured using two complementary experimental designs. First, a long-term monitoring (LTM) was set up in March 2003 in an homogeneous plot of forest of 100 m^2 (Fig. 1a–c; details in Limousin *et al.*, 2009). Second, *Q. ilex* trees were subjected to a rainfall exclusion experiment (RE) in 2009. Rainfall was excluded from two 195-m^2 forest plots (set up in 2007) from 1 February to 31 July 2009 (Fig. 1b,d,e), without changing other climate variables such as incident radiation, temperature and vapour pressure deficit. One plot was subjected to rainfall exclusion (RE_{Dry}) and one plot was used as reference (RE_{Ref}). A mobile rainfall shelter of 15 × 13 m sliding above the canopy was designed to trigger for any rainfall event over 0.25 mm (Fig. 1d; Misson *et al.*, 2010). Despite the shelter being designed to exclude nearly all the incoming rain, only 87% was excluded from RE_{Dry} (435 out of 491 mm) because of two power failures that delayed the movement of the roof (more details in Misson *et al.*, 2010).

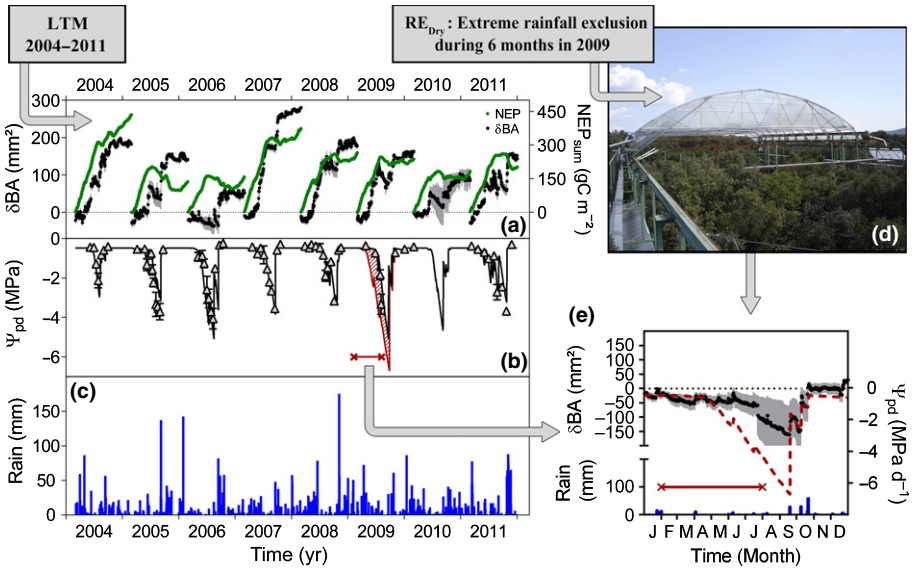

Fig. 1 Data and experimental set-up used in this study. Measurements were performed on the *Quercus ilex* forest of Puéchabon, France, using long-term monitoring (LTM) and rainfall exclusion (RE). (a) Net ecosystem productivity measured using the eddy covariance method (NEP_{sum}, solid green lines) and basal area increment (δBA, black points; error bar is SD between sampled trees) are shown as daily cumulative values. (b) Predawn water potential (Ψ_{pd}) observed (white triangles; error bar is SD) and extrapolated by simulation (solid black line). The solid red line framed by the crosses depicts the period of spring rainfall exclusion from 1 February 2009 to 31 July 2009 (b, e), the Ψ_{pd} simulated for this period is represented (solid red line, with hatched red area above). (c) Daily rain (blue bars). (d) Picture of the mobile shelter used for the RE. (e) Daily cumulative value of the basal area increment measured in tree subjected to the RE.

Table 1 Diameter at breast height (DBH) and stem density in *Quercus ilex* for the studied plots at Puéchabon, France (long-term monitoring plot, LTM, and the two rainfall exclusion plots: reference, RE_{Ref}, and exclusion, RE_{Dry}) for the years 2003 and 2007

	LTM 2003	LTM 2007	RE_{Ref} 2007	RE_{Dry} 2007
Quercus ilex				
Mean DBH (cm)	7.2 (2.65)	7.69 (2.55)	6.83 (2.78)	6.99 (2.65)
Mean DBH AD trees (cm)	11 (1.1)	11.4 (1.2)	10.8 (3.4)	8.8 (1.4)
Density (stem 100 m^{-2})	68	52	66	70

Means and SD in brackets are given for plots and stems followed by automatic dendrometers (AD).

In each monitored plot (LTM, RE_{Ref}, RE_{Dry}), six trees were selected and assessed for BA variations (Table 1). As the *Q. ilex* species exhibits very low wood growth at our site (Rodriguez-Calcerrada *et al.*, 2011), we selected trees that belong to the higher classes of DBH (> 7 cm) in order to ensure a stronger BA signal. From 2008 onwards, trees of the LTM experiment were pooled together with trees of the RE_{Ref} in order to increase sample size.

Stem circumference measurements

Stem circumference changes were recorded using AD (ELPA-98, University of Oulu, Oulu, Finland). The outer layer of dead bark was removed on each selected tree before setting up the AD 1.3 m aboveground. Band dendrometers are made of a potentiometer and a band of stainless steel (resolution < 27 µm, temperature sensitivity 1.65×10^{-5} mm^{-1} C^{-1}) connected to a data logger (model CR 1000; Campbell Scientific Ltd, Shepshed, UK). Measurements were recorded at a 30-min time-step resolution. The maximum daily value of circumference was recorded daily (typically happening around midnight). The daily circumferences were transformed and expressed in mm^2 to obtain daily basal area (δBA, in mm^2 d^{-1}). Analyses and graphs were performed with averaged δBA values of 6–12 individual trees expressed either in absolute or in relative to the maximal individual yearly BA.

Identification of the phenological stages of the seasonal pattern of stem growth

In order to identify the phenological stages of stem growth, we assumed that shrinking stems never lose wood volume; instead, they shrink as a result of decreasing water content in the elastic tissues of stem (mainly phloem) or of decomposing phloem tissues (Zweifel *et al.*, 2006).

For each tree and each year we estimated the different phenological stages that described the course of stem BA variations by analysing the pattern of cumulated daily variations of δBA (in mm^2) according to Zweifel *et al.* (2010; Fig. 2a). The

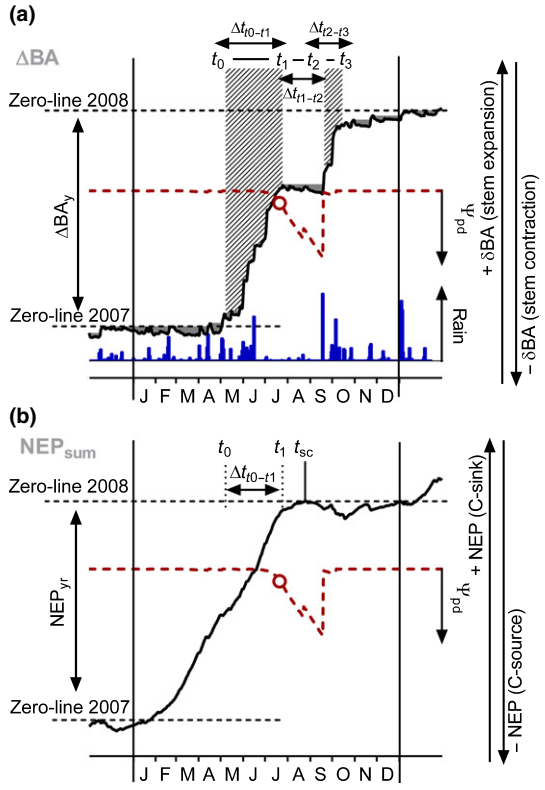

Fig. 2 Illustration of the method used for the data processing of automatic dendrometers (AD) and net carbon fluxes in *Quercus ilex*, following the approach of Zweifel *et al.* (2010). Data from 2007 has been used for the example. (a) Pattern of cumulated daily basal area variations (δBA). The stem water deficit (hatched areas), tree predawn water potential (Ψ_{pd}; red dashed line) and rainfall (Rain; blue bars) are indicated. The different phases of BA variations (Δt_{t0-t1}, Δt_{t1-t2}, Δt_{t2-t3}) are illustrated with the double arrows and the different stages of stem increment (onset of growth, t_0; summer interruption of growth, t_1; summer growth resumtion, t_2; autumn growth interuption, t_3) are reported. The zero-line of the current year is the culmination point of the past year. (b) Pattern of cumulated net ecosystem production (NEP_{sum}). The yearly NEP (NEP_{yr}) is the culminating point of the cumulated NEP from the culmination point of the past year (Zero-line 2007) to the culmination point of the current year (Zero-line 2008). The tree Ψ_{pd} is indicated by the red dotted line. t_{sc}, date when the ecosystem switches from carbon sink to source.

starting point of annual BA increment (hereafter t_0), noticeable from AD measurements, was defined as the first day at which BA exceeded the culmination point of the previous year (zero-line in Fig. 2a; Campelo *et al.*, 2007; Zweifel *et al.*, 2010) plus an error term σ_w specific to each year. This term σ_w corresponds to the variability of δBA out of the growing period and was set as the SD of δBA from early November to the end February (corresponding to the period when no significant trend on δBA was observed). The last day of spring growth (t_1) corresponds to the first day when δBA was null or negative. For more information on determination of t_0 and t_1, see Methods S2 and S3, Table S1 and Fig. S1.

A second growing period occurred in autumn bounded by t_2 and t_3. The beginning of this period (t_2) was defined as the first day when δBA was equal or higher than the δBA recorded at t_1. The end of this autumn BA increment period (t_3) was defined as the first day for which δBA was lower than the δBA recorded out of the increasing period (November–end February) minus σ_w.

The duration (Δt) and the variations of basal area (ΔBA) for the time periods of interest are subscripted with the following indices: $_{t0-t1}$, $_{t1-t2}$, $_{t2-t3}$ and $_{yr}$, for the period from t_0 to t_1, from t_1 to t_2, from t_2 to t_3, and for the whole year, respectively (Fig. 2a).

Ecosystem carbon flux measurements

Eddy covariance fluxes of CO_2, sensible heat, latent heat and momentum had been measured continuously since 2001 at the top of a 12-m-high tower that is *c.* 6 m above the canopy (more details in Methods S4). Our eddy covariance facility included a three-dimensional sonic anemometer (Solent R3; Gill Instruments, Lymington, UK) and a closed path infrared gas analyser (IRGA, model LI 6262; Li-Cor Inc., Lincoln, NE, USA), both sampling at a rate of 21 Hz. Processing schemes of Fluxnet have been used for filling data gaps and partitioning NEP into GPP and ecosystem respiration R_{eco} (Reichstein *et al.*, 2005; Papale *et al.*, 2006). The half-hourly fluxes were summed at yearly time steps for further analysis.

Both GPP and NEP were summed on a daily and yearly time step and for each period defined earlier (Δt_{t0-t1}, Δt_{t1-t2}, Δt_{t2-t3}; Fig. 2a). NEP was summed yearly (NEP_{yr}) over the period delimited as follows: onset, the first day when NEP was higher than the NEP maximum value of the previous year; ending, the maximum value of the year (Fig. 2b).

Environmental variables and predawn leaf water potential modelling

A standard weather station was located in a tree-free area, 230 m east of the eddy covariance tower; the station had provided long-term climatic data since 1984. Precipitation was measured with a tipping bucket rain gauge (ARG100; Environmental Measurements, Sunderland, UK) calibrated to 0.2 mm per tip and placed 1 m above the ground surface; air temperature was recorded with an MP100 sensor (Rotronic, Bassersdorf, Switzerland) and net radiation was measured with a pyranometer (SKS1110; Skye Instruments, Powys, UK), both at 2 m above the ground surface.

Soil water storage integrated over the rooting depth (i.e. 4.5 m, Rambal, 2011), was measured for the period 1984–1986 and then 1998 onwards, at approximately monthly intervals, using a neutron moisture gauge (Hoff *et al.*, 2002). Discrete measurements were interpolated at a daily time step with a soil water balance model (Rambal, 1993; Grote *et al.*, 2009) The drainage curve relating deep drainage to soil water storage depends on the stone content over the whole-soil profile (Rambal, 1990). The model was driven by daily values of incoming solar radiation, minimal and maximal temperature, and rain amount. Soil water storage and soil water potential were related by a Campbell-type retention curve (Campbell, 1985) whose parameters are strongly dependent on soil texture (Saxton *et al.*, 1986; see details in Rambal *et al.*, 2003). Comparison of measured against simulated values predawn leaf water potential, displayed very good

agreement: reduced major axis (RMA) regressions yielded an R^2 of 0.84, the slope was 0.93 ± 0.05 ($P < 0.0001$, $n = 54$), and the intercept was not significantly different from 0. Leaf water potential values came from discrete measurements performed on the study site (Limousin *et al.*, 2012). We used the simulations of predawn water potential rather than soil water content as it is much more closely related to plant water potential and therefore plant functioning (Rambal *et al.*, 2003). In order to characterize the interannual variations of water limitation, we computed a drought severity index, the water stress integral (WSI) defined by Myers (1988), as the yearly sum of predawn water potential.

Statistical analysis

We assessed the links between stem BA variations and stem phenology, climatic variable and ecosystem carbon fluxes by testing the correlations (Pearson) at the daily, monthly, seasonal (JFM, AMJ, JAS and OND) and annual timescales and for different growth periods. In order to assess whether the different stages of stem BA increment (see earlier) were driven by some particular environmental factors, we computed the correlations between the different growth stages and climatic variables (precipitation and temperature) aggregated at the monthly and the seasonal scales. See Methods S5 for additional information.

Spring increment period duration under climate projections

We finally investigated the climate change impacts on the length of the spring growing period (Δt_{t0-t1}). We used climate projections under the 'business as usual scenario' of the IPCC 2014 (IPCC-SRES A1B scenario) from a limited-area circulation model (LAM) and extracted the 8 × 8 km gridded daily data covering the Puéchabon study site. The LAM technique consists of nesting a limited-area circulation model – here the ALADIN-Climate model – inside a coarser global climate model (GCM) –here the CNRM ARPEGE-climate GCM (Colin *et al.*, 2010) – in order to deliver a more accurate reproduction of the climate at fine resolution. Daily temperatures, incoming solar global radiation and rain amount simulated by the ALADIN-Climate were used as input data in the water budget model described earlier to provide daily projections of the predawn water potential. Three 30-yr time-slices were retained: current period (1971–2000), near future (2021–2050) and remote future (2071–2100).

Results

Seasonal pattern of stem BA variations

At the seasonal scale, BA variations showed a pattern characterized by successive periods that can be circumscribed by four dates (Fig. 2a). Two periods of BA increase occurred in spring (Δt_{t0-t1}) and autumn (Δt_{t2-t3}). Δt_{t0-t1} was highly variable among years (44.5% of variations) and values ranged from null in 2006 to 78 d (SE = 7) in 2007 (Fig. 1a). Two periods without stem growth occurred in summer (Δt_{t1-t2}) and in winter between t_3 and t_0 of the following year. Δt_{t1-t2} lasted 81 d (SE = 10) on average but varied among years and was strongly correlated with the WSI ($r = 0.87$, $P < 0.05$). The dates t_0, t_1, t_2 and t_3 occurred on average in mid-May (day 135, SE = 4), early July (day 184, SE = 6), late September (day 264, SE = 6) and late October (day 296, SE = 3), respectively.

This bimodal pattern was found across all years except in 2006 (Fig. 1a), which was extremely dry (Table 2), with the lowest WSI recorded since 1984 (data not shown). This extreme drought was due to low rainfalls between March and August (142 mm vs average 296 mm) combined with high temperatures during the same period. This year, five trees out of six exhibited no positive variation of stem BA before 9 September (day 252). A single tree experienced a small spring increase (contributing to 17% of its annual growth this year) in stem growth that happened 1 d (7 May, day 127). Hence, t_0 and t_1 were not determined in 2006 and we considered that Δt_{t0-t1} was nil.

Yearly variations of growth characteristics

The yearly basal area increment (ΔBA_{yr}) exhibited important variations between years (CV = 37%; Fig. 1a). The ΔBA_{yr} of trees averaged 174 mm^2 (SE = 23), the minimal value was 65 mm^2

Table 2 Meteorological data and annual water deficit (water stress integral, WSI) in *Quercus ilex* for the studied period (2004–2011)

	Rain (mm)			T_{air}			WSI (MPa d^{-1})
Year	yr	AMJ	JAS	yr	JFM	JAS	yr
2004	990	234	213	12.95	6.10	20.70	−113
2005	832	178	277	12.92	5.41	21.12	−162
2006	952	53	299	14.07	5.74	22.33	−359
2007	682	289	126	13.79	8.41	20.41	−160
2008	1231	355	59	13.49	7.94	20.93	−187
2009	779	270	80	14.15	6.81	22.49	−279
2010	948	166	74	12.88	5.04	21.96	−246
2011	1164	114	123	14.45	7.30	21.51	−256

Sum of rainfall (rain), mean air temperature (T_{air}) and WSI are indicated for the whole year (yr), from January to March (JFM); April to June (AMJ) and from June to August (JJA).

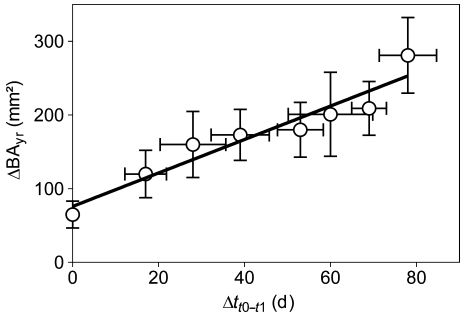

Fig. 3 Relationship between yearly basal area increment (ΔBA_{yr}) and the duration of the spring BA increment period (Δt_{t0-t1}; see Fig. 2a) ($R^2 = 0.91$; $P < 0.001$) in *Quercus ilex*. The bars depict the ± SE between sampled trees ($n = 6$ or 12).

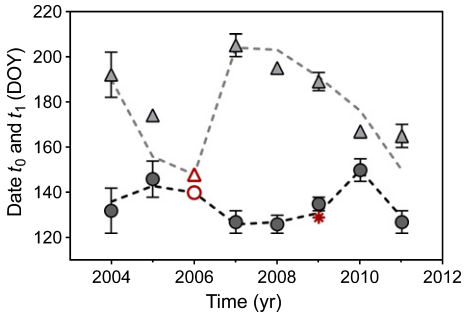

Fig. 4 Interannual variations of the spring onset of growth (t_0; circles) and the summer growth interruption (t_1; triangles) for observed (symbols) and predicted (dashed lines) values in *Quercus ilex*. t_0 and t_1 observed are depicted with dark grey circles and light grey triangles, respectively. The dark grey dotted line represent the t_0 predicted using a nonlinear relationship fitted between the onset t_0 and the mean January–March temperature (T_{JFM}): $t_0 = 849.2 \times \exp(-0.6436\, T_{JFM}) + 121$. R^2 and RMSE are 0.95 and 2.6 d, respectively. The light grey dotted line represents the t_1 predicted using the day of year (DOY) when a threshold plant water potential of −1.1 MPa was reached ($R^2 = 0.75$; RMSE = 7 d). In 2006 the early and strong drought precluded any observation of growth, but the predicted t_0 and t_1 are reported with a red circle and a red triangle, respectively. No growth was observed in trees subjected to the rainfall exclusion in 2009, and thus we reported the t_1 predicted (red asterisk) and the t_0 was taken from the control plots. The errors bars represent ± SE with $n = 6$ or 12.

(SE = 18) in 2006 and the maximal value was 282 mm^2 (SE = 51) in 2007 (Fig. 1a).

Most ΔBA_{yr} was achieved during spring (Figs 1a, 2a). ΔBA_{t0-t1} averaged 67% of ΔBA_{yr} over the study period, the remaining increment being achieved in autumn (ΔBA_{t2-t3}). The yearly variations of ΔBA_{yr} were principally driven by the length of the spring growing period (Δt_{t0-t1}) as evidenced by the close relationship between ΔBA_{yr} and Δt_{t0-t1} (Fig. 3; $r = 0.96$, $P < 0.001$). The correlation between ΔBA_{yr} and Δt_{t2-t3} was not significant ($P = 0.38$; Table S2).

The stage t_0 was correlated with mean temperature from January to March ($r = -0.91$; Table S3). A decreasing exponential model between mean January–March temperature and t_0 was the best model that described this correlation (Fig. S2).

The stage t_1 was positively correlated with the sum of precipitations from April to June ($r = 0.82$, $P < 0.01$, Table S3). By exploring the role of predawn water potential (Ψ_{pd}) in determining t_1, we found that stem increment interrupted in summer for a threshold value of Ψ_{pd}, $\Psi_{t1} = -1.1$ MPa (RMSE = 7 d, Fig. S1). Using this Ψ_{t1}, the relationship between predicted and observed t_1 was highly significant ($P < 0.01$, $R^2 = 0.75$), with a slope of 1 and an intercept not significantly different from 0. However, a substantial uncertainty was observed in the predictions of t_1 as we found very close results for Ψ_{t1} values ranging between −1.1 and −1.3 MPa (see Methods S3 and Fig. S1).

Using the relationship between t_0 and temperature, and the relationship between t_1 and Ψ_{pd}, we simulated the dates t_0 and t_1 over the period 2004–2011 (Fig. 4). In 2006, the year when no spring growth was observed (see earlier), t_0 would have occurred on day 140 and t_1 on day 148 according to the model (Fig. 4).

Stem BA variations in response to a rainfall exclusion experiment

The rainfall exclusion experiment (RE_{Dry}) was carried out from 1 February to 31 July 2009 and led to an unusually long period of water deficit. The simulated predawn water potential (Ψ_{pd}) dropped very early in the excluded plot compared with the control treatment (Fig. 1b, see also Misson *et al.*, 2010). According to the water budget simulations, Ψ_{pd} reached the threshold Ψ_{t1} in early May (between days 126 and 131; Fig. 4) and remained *c.* 155 d below Ψ_{t1} (Fig. 1e). In the trees monitored by AD, Δt_{t0-t1} was null and no growth was observed in spring. The stem shrinkage during the summer reached 2.4 and 0.7% of the total stem BA for the RE_{dry} and LTM plots in 2009, respectively. After the first autumnal rainfall events, no significant basal area increment was observed (i.e. most trees remained below the zero line; Fig. 1e). The annual increase in stem basal area of trees subjected to RE_{Dry} was very low ($\Delta BA_{yr} = 47$ mm^2, SE = 15; Fig. 1e), significantly lower ($P < 0.05$) than for trees in the control treatment (131 mm^2, SE = 31; Fig. 1a), and even lower than the lowest value observed for the whole time period during the extremely dry year 2006 (Fig. 1a).

Relationships between growth, fluxes and environmental factors at different timescales

The correlation between ecosystem carbon fluxes and stem increment decreased with increasing temporal resolution (Table 3). At the yearly timescale, the stem basal area increment (ΔBA) was positively and highly correlated with carbon fluxes of ecosystem (NEP, GPP and Reco with $r = 0.87$, 0.81 and 0.78, respectively, Table 3). At the seasonal and monthly timescales, the GPP and Reco remained positively correlated with ΔBA but the magnitude of the correlation (r) decreased drastically to 0.63 and 0.72 at seasonal and to 0.44 and 0.62 at monthly timescales, respectively (Table 3). We also noticed that the correlation between ΔBA and NEP became nonsignificant (Table 3) at these two temporal scales. At the daily timescale, the correlations between ecosystem carbon fluxes and stem increment were still significant but the coefficients were much closer to 0 (Table 3). At a daily timescale, carbon fluxes and stem increment exhibited specific responses to temperature and Ψ_{pd} (Figs 5a,b, S3). δBA depicted a parabolic-like response to temperature (Fig. 5b). δBA was almost always positive between 5 and 25°C. Below 5 or > 25°C δBA was nil, and even negative below 0 or above 28°C. NEP showed a similar pattern but remained positive for a larger range of temperatures (0 to 28°C). The GPP depicted a similar shape but always remained positive. Stem BA growth and ecosystem carbon fluxes were both highly sensitive to Ψ_{pd} (Fig. 5b). δBA rapidly decreased as Ψ_{pd} decreased, and reached zero for the plant water potential threshold we identified ($\Psi_{t1} = -1.1 \pm 0.1$ MPa). The NEP decreased with Ψ_{pd} but became negative (ecosystem became a net source of CO_2) only for values of Ψ_{pd} greatly below Ψ_{t1} at *c.* −2.7 MPa. At a lower rate, GPP also decreased with decreasing Ψ_{pd} but remained above 0 even for very low water potentials (< −4 MPa).

Table 3 Correlations at different timescales between basal area increment (BA), net ecosystem photosynthesis (NEP), gross primary productivity (GPP) and respiration of ecosystem (R_{eco}) in *Quercus ilex*

	Yearly		Seasonally		Monthly		Daily	
BA (mm^2) vs	*r*	*P*-value	*r*	*P*-value	*r*	*P*-value	*r*	*P*-value
NEP ($gC\ m^{-2}\ j^{-1}$)	**0.87**	0.0045	0.27	0.135	4.10^{-4}	0.997	**−0.23**	< 0.0001
GPP ($gC\ m^{-2}\ j^{-1}$)	**0.81**	0.0156	**0.63**	0.000	**0.44**	< 0.0001	**−0.06**	0.001
R_{eco} ($gC\ m^{-2}\ j^{-1}$)	**0.78**	0.0215	**0.72**	< 0.0001	**0.62**	< 0.0001	**0.18**	< 0.0001

Correlations were carried between sums of daily values calculated yearly, seasonally and monthly for 8 yr (2004–2011). The coefficient of correlation (*r*) and *P*-value are given. Negative correlations are indicated by (–), and significant correlations ($P < 0.05$) are in bold.

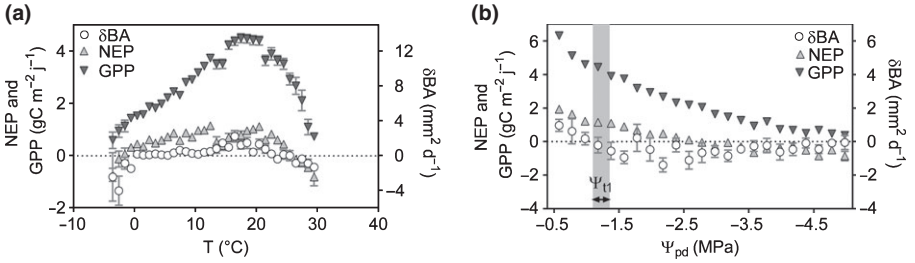

Fig. 5 Function of response of daily stem basal area variations (δBA, white circles), daily gross primary productivity (GPP, dark grey inverted triangles) and daily net ecosystem productivity (NEP, light grey triangles) to (a) air temperature (*T*) and (b) simulated predawn water potential (Ψ_{pd}) in *Quercus ilex*. For (a) the daily data were averaged for each 1°C step of temperature. For (b) only the data for the spring growing period and the summer growth-interruption period (Δt_{t0-t1} and Δt_{t1-t2}; see Fig. 2a) were taken and binned for 0.2 MPa step of Ψ_{pd}. The estimated predawn leaf potential of growth cessation (Ψ_{t1}) is represented by a grey area; ± SE are represented.

At the annual scale, we found a good correlation between the index of water stress (WSI) and NEP, the R^2 of the linear relationship between NEP_{yr} and the WSI was 0.81 ($P < 0.05$; Fig. S3). To a lower extent, WSI was also linearly related to the stem basal area increment (ΔBA_{yr}, $R^2 = 0.53$, $P < 0.05$; Fig. S3), however, the slope of the linear relationship became not significantly different from 0 when the very dry year 2006 was removed ($P = 0.29$). The best explanatory variable for the annual stem increment (ΔBA_{yr}) was the length of the spring growing period ($r = 0.96$; Table S2) as evidenced by the linear relationship between Δt_{t0-t1} and ΔBA_{yr} ($\Delta BA_{yr} = 2.27 \times \Delta t_{t0-t1} + 75.58$, $R^2 = 0.91$; Fig. 4). Similarly, spring basal area increment (ΔBA_{t0-t1}) was correlated with NEP_{t0-t1} ($r = 0.81$; Table 3) but the correlation was better with Δt_{t0-t1} ($r = 0.90$; Table S2). On the contrary, the autumn basal area increment (ΔBA_{t2-t3}) was well correlated with NEP_{yr} and NEP_{t0-t1}, but not with the time elapsed during the autumn basal area increase (Δt_{t2-t3}; Table S2), suggesting an overriding role of the spring conditions in the amount of growth achieved in autumn.

Projection of spring growth duration under climate change scenario

We provide the time courses of yearly rainfall amounts, potential evaporation and the mean air temperature for the three time-slices in the Supporting Information (Table S4). The climate projection predicted a regular increase in potential evaporation as a result of higher temperature from the current period to the remote future period. Whereas yearly rainfalls were predicted to remain constant for the near future period, a marked decrease in summer rainfall was projected for the remote future period. The length of the spring growing period (Δt_{t0-t1}) simulated for the current period (1971–2010) was 48 d on average. Δt_{t0-t1} was predicted to increase up to 50 d for the near future period (2021–2050) as a result of an earlier t_0 (Fig. 6). Earlier t_0 resulted from an increase in the projected winter temperature from the current period to the near future period. In fact, t_1 was not much affected

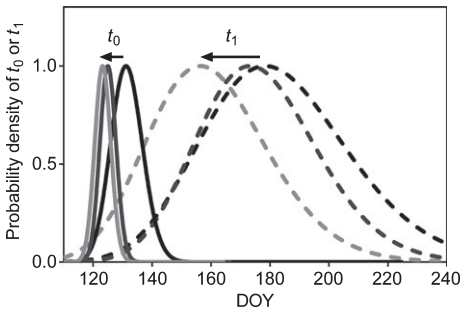

Fig. 6 Probability densities of stages t_0 (spring onset of growth) and t_1 (summer interruption of growth) under current and future climate in *Quercus ilex*. Projections were obtained using a simulated climate for historical conditions (1971–2000, black solid/dashed lines), or under a climate change scenario (IPCC, 2014, A1B) for the mid-century (2031–2060, dark grey solid/dashed lines) and late century (2071–2100, light grey solid/dashed lines). t_0 distributions (solid lines) were predicted as a function of the mean January–March temperature (T_{JFM}) using the following equation: $t_0 = 849.2 \times \exp(-0.6436\ T_{JFM}) + 121$ (see Fig. 4); t_1 distribution (dashed lines) was determined as the first day when the water potential fell below −1.1 MPa (see Fig. 4). Arrows indicate the direction of the changes in the median of t_0 and t_1 from current to future climate. DOY, day of year.

for the near future period (Fig. 6), as little changes in rainfall and therefore in the projected water deficit were predicted by the climate model for the near future period (not shown). Conversely, an opposite trend was projected in the remote future period (2071–2100) and Δt_{f0-t1} decreased to 40 d on average mainly due to an earlier t_1. The distribution of t_1 shifted by 15 d between the near future and the remote future period (Fig. 6) due to an earlier and more intense water deficit projected for the end of century (not shown). Despite the continuous increase in temperature from the near future to the remote future period, the distribution of t_0 shifted only 3 d earlier (Fig. 6); this was the result of the nonlinearity of the relationship between January–March temperature and t_0 (Fig. S2).

Discussion

Correlations between BA increment and carbon fluxes

We found a close relationship between different ecosystem carbon fluxes cumulated over the year (GPP_{yr}, NEP_{yr}) and the cumulated variations of BA over the year (ΔBA_{yr}) (Table 3). This is in agreement with the strong correlations between growth and carbon gain reported at larger spatial and temporal scales that legitimate the representation of growth as a constant fraction of GPP in most vegetation models (Litton *et al.*, 2007). The relationship between carbon fluxes and growth remain highly significant at all timescales and reinforce the idea that tree water relations and stem growth information contained in AD signal are indicative for forest productivity as proposed by Zweifel *et al.* (2010). However, contrary to the findings of Zweifel *et al.* (2010), the strength of the correlation became drastically less important when the temporal resolution was decreased from the annual to the daily timescale. It may be that the strong seasonal variations of water deficit and temperature that are typical of the Mediterranean climate of our site have affected stem basal area variations and carbon fluxes differently at high temporal resolution. This hypothesis is supported by the observed stem increment and carbon fluxes responded differently to temperature and water deficit (Fig. 5a,b). Indeed, a synchronization of the responses to temperature of stem increment and carbon gain was observable only for temperatures ranging between 5 and 25°C (Fig. 5a). Below 5°C the stem increment was close to 0 whereas GPP remained positive. This decoupling is congruent with the knowledge that the different processes involved in wood formation (cell division–elongation) are far more sensitive than photosynthesis to cold stress (Körner, 2003, 2006). We also observed that daily GPP decreased continuously with decreasing predawn water potential (i.e. increasing water stress), whereas stem increment decreased sharply until −1.1 MPa and then remained mostly nil and invariant for values of Ψ_{pd} ranging from −1.1 to −4 MPa (Fig. 5b). These observations are also consistent with the premise that growth stops before stomata are fully closed and before cavitation occurs (Delzon & Cochard, 2014; Martin-StPaul *et al.*, 2014), and that processes involved in secondary growth are more sensitive than photosynthesis to water deficit (Hsiao & Acevedo, 1974; Hsiao & Xu, 2000; Körner, 2003; Daudet *et al.*, 2005; Muller *et al.*, 2011). Interestingly, when stem increment was nil, during the periods of low temperature or high water stress, the NEP frequently remained positive (i.e. the whole ecosystem is a carbon sink; Figs 1a, 5a,b). Consequently, it is unlikely that a lack of available substrate (caused by higher respiration rates than photosynthesis) was responsible for the decrease of stem increment we observed during summer and winter period. This conclusion is also supported by the recent study of Rodríguez-Calcerrada *et al.* (2014) conducted on the same site, which showed that the nonstructural carbohydrate content of the sapwood and phloem tended to increase with the seasonal increase in water deficit. Other possible destinations for the carbon sequestered during the growth interruption period need further investigation. Among the different possible destinations, this carbon, if not consumed by maintenance respiration, may be allocated preferentially to organs close to the source as proposed by Woodruff & Meinzer (2011) (e.g. growth, leaves and reproductive organs), used for the maturation of the tissue produced during the previous weeks (see Babst *et al.*, 2014) or used to repair or build organs involved in water resource acquisition and transport such as fine roots or xylem (Brodribb *et al.*, 2010).

Overall, these results indicate that part of stem increments at fine temporal resolution is driven by the climatic constraints rather than by the carbon gain. We must, however, acknowledge that the complexity of the information contained in the AD signal may blur our conclusions. Indeed, if in the case of a long-term integration period (e.g. year), growth-related processes likely form the dominant part of the AD signal (Steppe *et al.*, 2006; Zweifel *et al.*, 2006), at higher temporal resolution the AD signal is the product not only of wood growth (cell enlargement), but also of water-related processes and phloem size changes (Zweifel *et al.*, 2006). Moreover, probable lag effects between carbon uptake at the leaf level and wood production further down the stem (e.g. Gessler *et al.*, 2014), may blur the correlation between fluxes and BA growth at short timescales. Hence, it is likely that the deterioration of the correlations between stem BA variations and fluxes is also related to nongrowth components. However, we will discuss in the following how the seasonal timing of tree basal area variations seems to exert a tight control over annual stem growth, which also seems to be under the control of temperature and water deficit.

Spring conditions as the main drivers of *Q. ilex* annual growth

Yearly BA increment showed biphasic growth pattern over the year, which is congruent with studies on *Q. ilex* stem growth (Campelo *et al.*, 2007; Montserrat-Marti *et al.*, 2009; Gutiérrez *et al.*, 2011) and those on other Mediterranean tree species (e.g. Camarero *et al.*, 2010). Despite this pattern, the spring growing period was the main driver of the annual stem basal area growth as shown by the relationship between the length of the spring growing period and the annual BA increment (Fig. 3). The intercept of this relationship defines a residual autumnal growth observed in 2006 when the important and early drought prevented any spring growing period (Fig. 1a,b). Such residual

growth may have resulted either from an autumnal cambial activity (i.e. cell formation and expansion) or from the enlargement of cells produced during spring. The latter hypothesis is supported by the results from the rainfall exclusion experiment as trees in the exclusion plot did not grow at all – even after soil had returned to field capacity following autumnal rainfall (Fig. 1e) – whereas trees under ambient conditions showed a substantial increment (Fig. 1a). These results are consistent with an early determinism of most of the stem increment (i.e. before drought has occurred), and it may be that most cambial activity happened during spring. In 2006, spring cambial activity was probably insufficient to be detected in the noisy signal of dendrometers, only a residual autumnal growth was observed. Overall, the idea that spring conditions control the annual stem enlargement to a large extent is in line with robust correlations between spring carbon sequestration and annual growth evidenced in temperate forest (Granier *et al.*, 2008; Babst *et al.*, 2014). Under temperate climate, the summer interruption of stem growth has been related to changes in day length (Rossi *et al.*, 2006; Camarero *et al.*, 2010), but in our case the good relationship between t_1 and the predawn water potential support the idea that water deficit plays a crucial role in determining the interruption of stem growth (Fig. 3).

Drivers of the spring onset and the summer cessation of stem increment

The spring BA increment duration (Δt_{t0-t1}) is determined by the onset and interruption of spring BA increment (t_0 and t_1, respectively; Table 3). To understand what drives the interannual variations of Δt_{t0-t1}, we isolated those factors controlling t_0 and t_1.

The onset of BA increment (t_0) was closely linked to the mean temperature from January to March (Fig. S2). This is in agreement with several studies reporting that the onset basal growth is highly responsive to temperature (Körner, 2006; Rossi *et al.*, 2007, 2008, 2011; Deslauriers *et al.*, 2008; Swidrak *et al.*, 2011). The minimum daily temperature during the week preceding t_0 was never $< 5°C$, which is in agreement with a daily minimum threshold temperature ranging between 4 and 7°C, previously reported in other tree species (Rossi *et al.*, 2007, 2008; Deslauriers *et al.*, 2008; Swidrak *et al.*, 2011).

The summer BA increment cessation is frequently reported for Mediterranean trees and is discussed as a period of quiescence of cambial activity induced by water limitation (Campelo *et al.*, 2007; Montserrat-Marti *et al.*, 2009; Camarero *et al.*, 2010; Gutiérrez *et al.*, 2011). In this study, water deficit played a critical role in the timing of summer increment BA cessation (t_1) as evidenced by the positive correlation between the amount of rainfall in spring and t_1 (Table S3). More importantly, we found a close relationship between t_1 and the date when predawn plant water potential reached a threshold plant water potential of −1.1 MPa (thereafter Ψ_{t1}; Fig. S1). This threshold value provides a link between BA increment cessation at the tree scale and environmental conditions (influenced by climate and soil). As discussed earlier, it is acknowledged that the processes involved in wood growth are highly sensitive to water deficit (Hsiao & Xu, 2000; Muller *et al.*, 2011). Lockhart (1965) formalized the reduction of plant cell growth in water deficit conditions by a decrease of the pressure required for cell enlargement (the turgor pressure) below a critical value. The turgor pressure depends on both the hydrostatic pressure, which itself depends on hydraulic conductance, and the cell solute potential that relies on accumulation of osmolytes within the cell medium (Hsiao & Xu, 2000). Ψ_{t1} may therefore approximate the plant water potential that precludes any osmotic adjustments to maintain a turgor pressure allowing cell growth.

Identification of the factors controlling t_0 and t_1 allows us to predict stem growth duration which is highly correlated with annual stem growth (Fig. 3). We acknowledge that our approach to predicting stem growth is simple and neglects important factors such as the delayed effects of drought (Granier *et al.*, 2008), changes in allocation pattern due to mast seeding (Mund *et al.*, 2010) or age-related changes in tree allometry (Magnani *et al.*, 2002). However, despite these challenges, the Δt_{t0-t1} simulated for the past 40 yr explained *c.* 40% of variation of yearly tree ring width sampled at our site ($P < 0.0001$, data not shown).

Implication for vegetation models

Overall these results suggest that at our site stem growth is limited more by a decrease of the sink activity (sink limitation) due to low temperature and high water deficit, than by a decreased availability of carbon substrate (source limitation). By projecting these simple rules under a climate change scenario, we found an important reduction of the average Δt_{t0-t1} for the remote period (2071–2100) mostly due to an earlier interruption of increment associated with a 15 d shift in the date t_1 (Fig. 6), that may translate into a decrease in stem growth (Fig. 3). This latter result is in agreement with the shift towards an earlier drought season projected by Ruffault *et al.* (2014) using a water balance model along with climate projection under the A1B scenario in southern France. The decrease in growth we projected for the end of the century contrasts markedly with projections performed at our site with an ecophysiological process-oriented model that reported an increase in *Q. ilex* growth for the end of the century with the same climate scenario, mostly as a result of a positive feedback between increasing atmospheric CO_2 concentration and photosynthesis and productivity (Davi *et al.*, 2006). Our projections of tree water potential must be considered cautiously as they do not account for acclimation mechanisms to drought (e.g. plant allometry, hydraulic conductivity, leaf area index, stem density) that may dampen the increase in tree water stress in a dryer future (Barbeta *et al.*, 2013, 2014; Martin-StPaul *et al.*, 2013). We must also acknowledge that higher winter temperature may compensate for the shorter growing season by stimulating cell divisions, expansion and maturation rates (see, for instance, Rossi *et al.*, 2014). However, integrating such sink limitation mechanisms in ecophysiological process-oriented models of forest functioning can help refining the projections of climate change outcomes on forests.

Acknowledgements

This work was supported by the French Environment and Energy Management Agency (ADEME) and the DROUGHT+ (ANR-06-VULN-003-01). Additional support was provided by CARBO-Extreme (FP7-ENV-2008-1-226701). The authors would like to thank Christian Collin, David Degueldre and Raquel Rodriguez for their assistance with the installation of the experimental setup. We also thank Jésus Rodriguez-Calcerrada, Joannès Guillemot and Nicolas Delpierre for helpful discussions and comments on an earlier version of the manuscript.

References

Babst F, Bouriaud O, Papale D, Gielen B, Janssens IA, Nikinmaa E, Ibrom A, Wu J, Bernhofer C, Köstner B. 2014. Above-ground woody carbon sequestration measured from tree rings is coherent with net ecosystem productivity at five eddy-covariance sites. *New Phytologist* **201**: 1289–1303.

Barbeta A, Mejía-Chang M, Ogaya R, Voltas J, Dawson TE, Peñuelas J. 2014. The combined effects of a long-term experimental drought and an extreme drought on the use of plant-water sources in a Mediterranean forest. *Global Change Biology* **21**: 1213–1225.

Barbeta A, Ogaya R, Peñuelas J. 2013. Dampening effects of long-term experimental drought on growth and mortality rates of a Holm oak forest. *Global Change Biology* **19**: 3133–3144.

Bigler C, Bugmann H. 2003. Growth-dependent tree mortality models based on tree rings. *Canadian Journal of Forest Research* **33**: 210–221.

Bonan GB. 2008. Forests and climate change: forcings, feedbacks, and the climate benefits of forests. *Science* **320**: 1444–1449.

Boyer WD. 1970. Shoot growth patterns of young Loblolly pine. *Forest Science* **16**: 472–482.

Brodribb TJ, Bowman DJMS, Nichols S, Delzon S, Burlett R. 2010. Xylem function and growth rate interact to determine recovery rates after exposure to extreme water deficit. *New Phytologist* **188**: 533–542.

Camarero JJ, Olano JM, Parras A. 2010. Plastic bimodal xylogenesis in conifers from continental Mediterranean climates. *New Phytologist* **185**: 471–480.

Campbell GS. 1985. *Soil physics with basic: transport models for soil–plant systems.* Amsterdam, the Netherlands: Elsevier.

Campelo F, Nabais C, Freitas H, Gutiérrez E. 2007. Climatic significance of tree-ring width and intra-annual density fluctuations in *Pinus pinea* from a dry Mediterranean area in Portugal. *Annals of Forest Science* **64**: 229–238.

Cheaib A, Badeau V, Boe J, Chuine I, Delire C, Dufrêne E, François C, Gritti ES, Legay M, Pagé C. 2012. Climate change impacts on tree ranges: model intercomparison facilitates understanding and quantification of uncertainty. *Ecology Letters* **15**: 533–544.

Colin J, Déqué M, Radu R, Somot S. 2010. Sensitivity study of heavy precipitation in limited area model climate simulations: influence of the size of the domain and the use of the spectral nudging technique. *Tellus A* **62**: 591–604.

Daudet F-A, Améglio T, Cochard H, Archilla O, Lacointe A. 2005. Experimental analysis of the role of water and carbon in tree stem diameter variations. *Journal of Experimental Botany* **56**: 135–144.

Davi H, Dufrêne E, Francois C, Le Maire G, Loustau D, Bosc A, Rambal S, Granier A, Moors E. 2006. Sensitivity of water and carbon fluxes to climate changes from 1960 to 2100 in European forest ecosystems. *Agricultural and Forest Meteorology* **141**: 35–56.

Delzon S, Cochard H. 2014. Recent advances in tree hydraulics highlight the ecological significance of the hydraulic safety margin. *New Phytologist* **203**: 355–358.

Deslauriers A, Rossi S, Anfodillo T, Saracino A. 2008. Cambial phenology, wood formation and temperature thresholds in two contrasting years at high altitude in southern Italy. *Tree Physiology* **28**: 863–871.

Diffenbaugh NS, Giorgi F. 2012. Climate change hotspots in the CMIP5 global climate model ensemble. *Climatic Change* **114**: 813–822.

Dobbertin M. 2005. Tree growth as indicator of tree vitality and of tree reaction to environmental stress: a review. *European Journal of Forest Research* **124**: 319–333.

Fatichi S, Leuzinger S, Körner C. 2014. Moving beyond photosynthesis: from carbon source to sink-driven vegetation modeling. *New Phytologist* **201**: 1086–1095.

Gao X, Giorgi F. 2008. Increased aridity in the Mediterranean region under greenhouse gas forcing estimated from high resolution simulations with a regional climate model. *Global and Planetary Change* **62**: 195–209.

Gaucherel C, Guiot J, Misson L. 2008. Changes of the potential distribution area of French Mediterranean forests under global warming. *Biogeosciences* **5**: 1493–1504.

Gea-Izquierdo G, Fernandez-de-Una L, Canellas I. 2013. Growth projections reveal local vulnerability of Mediterranean oaks with rising temperatures. *Forest Ecology and Management* **305**: 282–293.

Gessler A, Ferrio JP, Hommel R, Treydte K, Werner RA, Monson RK. 2014. Stable isotopes in tree rings: towards a mechanistic understanding of isotope fractionation and mixing processes from the leaves to the wood. *Tree Physiology* **34**: 796–818.

Granier A, Bréda N, Longdoz B, Gross P, Ngao J. 2008. Ten years of fluxes and stand growth in a young beech forest at Hesse, North-eastern France. *Annals of Forest Science* **65**: 1.

Grote R, Lavoir A-V, Rambal S, Staudt M, Zimmer I, Schnitzler J-P. 2009. Modelling the drought impact on monoterpene fluxes from an evergreen Mediterranean forest canopy. *Oecologia* **160**: 213–223.

Gutiérrez E, Campelo F, Camarero JJ, Ribas M, Muntán E, Nabais C, Freitas H. 2011. Climate controls act at different scales on the seasonal pattern of *Quercus ilex* L. stem radial increments in NE Spain. *Trees* **25**: 637–646.

Hoff C, Rambal S, Joffre R. 2002. Simulating carbon and water flows and growth in a Mediterranean evergreen *Quercus ilex* coppice using the FOREST-BGC model. *Forest Ecology and Management* **164**: 121–136.

Hsiao TC, Acevedo E. 1974. Plant responses to water deficits, water-use efficiency, and drought resistance. *Agricultural Meteorology* **14**: 59–84.

Hsiao TC, Xu LK. 2000. Sensitivity of growth of roots versus leaves to water stress: biophysical analysis and relation to water transport. *Journal of Experimental Botany* **51**: 1595–1616.

IPCC. 2014. Barros VR, Field CB, Dokken DJ, Mastrandrea MD, Mach KJ, Bilir TE, Chatterjee M, Ebi KL, Estrada YO, Genova RC *et al.*, eds. *Climate change 2014: impacts, adaptation, and vulnerability. Part B: regional aspects. Contribution of Working Group II to the fifth assessment report of the Intergovernmental Panel on Climate Change.* Cambridge, UK & New York, NY, USA: Cambridge University Press.

Keenan T, Maria Serra J, Lloret F, Ninyerola M, Sabate S. 2011. Predicting the future of forests in the Mediterranean under climate change, with niche-and process-based models: CO_2 matters!. *Global Change Biology* **17**: 565–579.

Körner C. 2003. Carbon limitation in trees. *Journal of Ecology* **91**: 4–17.

Körner C. 2006. *Significance of temperature in plant life.* Oxford, UK: Blackwell Publishing Ltd.

Lévesque M, Saurer M, Siegwolf R, Eilmann B, Brang P, Bugmann H, Rigling A. 2013. Drought response of five conifer species under contrasting water availability suggests high vulnerability of Norway spruce and European larch. *Global Change Biology* **19**: 3184–3199.

Limousin JM, Rambal S, Ourcival JM, Rocheteau A, Joffre R, Rodriguez-Cortina R. 2009. Long-term transpiration change with rainfall decline in a Mediterranean *Quercus ilex* forest. *Global Change Biology* **15**: 2163–2175.

Limousin JM, Rambal S, Ourcival JM, Rodriguez-Calcerrada J, Perez-Ramos IM, Rodriguez-Cortina R, Misson L, Joffre R. 2012. Morphological and phenological shoot plasticity in a Mediterranean evergreen oak facing long-term increased drought. *Oecologia* **169**: 565–577.

Litton CM, Raich JW, Ryan MG. 2007. Carbon allocation in forest ecosystems. *Global Change Biology* **13**: 2089–2109.

Lockhart JA. 1965. An analysis of irreversible plant cell elongation. *Journal of Theoretical Biology* **8**: 264–275.

Magnani F, Grace J, Borghetti M. 2002. Adjustment of tree structure in response to the environment under hydraulic constraints. *Functional Ecology* **16**: 385–393.

Martin-StPaul NK, Limousin JM, Vogt-Schilb H, Rodríguez-Calcerrada J, Rambal S, Longepierre D, Misson L. 2013. The temporal response to drought

in a Mediterranean evergreen tree: comparing a regional precipitation gradient and a throughfall exclusion experiment. *Global Change Biology* **19**: 2413–2426.

Martin-StPaul NK, Longepierre D, Huc R, Delzon S, Burlett R, Joffre R, Rambal S, Cochard H. 2014. How reliable are methods to assess xylem vulnerability to cavitation? The issue of "open vessel" artifact in oaks. *Tree Physiology* **34**: 894–905.

Misson L, Limousin J-M, Rodriguez R, Letts MG. 2010. Leaf physiological responses to extreme droughts in Mediterranean *Quercus ilex* forest. *Plant, Cell & Environment* **33**: 1898–1910.

Montserrat-Marti G, Camarero JJ, Palacio S, Perez-Rontome C, Milla R, Albuixech J, Maestro M. 2009. Summer-drought constrains the phenology and growth of two coexisting Mediterranean oaks with contrasting leaf habit: implications for their persistence and reproduction. *Trees-Structure and Function* **23**: 787–799.

Muller B, Pantin F, Génard M, Turc O, Freixes S, Piques M, Gibon Y. 2011. Water deficits uncouple growth from photosynthesis, increase C content, and modify the relationships between C and growth in sink organs. *Journal of Experimental Botany* **62**: 1715–1729.

Mund M, Kutsch W, Wirth C, Kahl T, Knohl A, Skomarkova M, Schulze E-D. 2010. The influence of climate and fructification on the inter-annual variability of stem growth and net primary productivity in an old-growth, mixed beech forest. *Tree Physiology* **30**: 689–704.

Myers BJ. 1988. Water stress integral – a link between short-term stress and long-term growth. *Tree Physiology* **4**: 315–323.

Pan Y, Birdsey RA, Fang J, Houghton R, Kauppi PE, Kurz WA, Phillips OL, Shvidenko A, Lewis SL, Canadell JG *et al.* 2011. A large and persistent carbon sink in the world's forests. *Science* **333**: 988–993.

Papale D, Reichstein M, Aubinet M, Canfora E, Bernhofer C, Kutsch W, Longdoz B, Rambal S, Valentini R, Vesala T. 2006. Towards a standardized processing of net ecosystem exchange measured with eddy covariance technique: algorithms and uncertainty estimation. *Biogeosciences* **3**: 571–583.

Rambal S. 1990. Les transferts d'eau dans le systeme sol-plante en region mediterraneenne karstique: une approche hierarchique. PhD thesis, Université Paris 11, Paris, France.

Rambal S. 1993. The differential role of mechanisms for drought resistance in a Mediterranean evergreen shrub: a simulation approach. *Plant, Cell & Environment* **16**: 35–44.

Rambal S. 2011. Le paradoxe hydrologique des écosystèmes méditerranéens. *Annales de la Société d'Horticulture et d'Histoire Naturelle de l'Hérault* **2011**: 61–67.

Rambal S, Joffre R, Ourcival JM, Cavender-Bares J, Rocheteau A. 2004. The growth respiration component in eddy CO_2 flux from a *Quercus ilex* mediterranean forest. *Global Change Biology* **10**: 1460–1469.

Rambal S, Ourcival JM, Joffre R, Mouillot F, Nouvellon Y, Reichstein M, Rocheteau A. 2003. Drought controls over conductance and assimilation of a Mediterranean evergreen ecosystem: scaling from leaf to canopy. *Global Change Biology* **9**: 1813–1824.

Rambal S, Lempereur M, Limousin JM, Martin-StPaul NK, Ourcival JM, Rodríguez-Calcerrada J. 2014. How drought severity constrains gross primary production (GPP) and its partitioning among carbon pools in a *Quercus ilex* coppice? *Biogeosciences* **11**: 6855–6869.

Reichstein M, Falge E, Baldocchi D, Papale D, Aubinet M, Berbigier P, Bernhofer C, Buchmann N, Gilmanov T, Granier A. 2005. On the separation of net ecosystem exchange into assimilation and ecosystem respiration: review and improved algorithm. *Global Change Biology* **11**: 1424–1439.

Richardson AD, Carbone MS, Keenan TF, Czimczik CI, Hollinger DY, Murakami P, Schaberg PG, Xu X. 2013. Seasonal dynamics and age of stemwood nonstructural carbohydrates in temperate forest trees. *New Phytologist* **197**: 850–861.

Rocha AV, Goulden ML, Dunn AL, Wofsy SC. 2006. On linking interannual tree ring variability with observations of whole-forest CO_2 flux. *Global Change Biology* **12**: 1378–1389.

Rodríguez-Calcerrada J, Martin-StPaul NK, Lempereur M, Ourcival J-M, Carmen del Rey Md, Joffre R, Rambal S. 2014. Stem CO_2 efflux and its contribution to ecosystem CO_2 efflux decrease with drought in a Mediterranean forest stand. *Agricultural and Forest Meteorology* **195–196**: 61–72.

Rodriguez-Calcerrada J, Perez-Ramos IM, Ourcival JM, Limousin JM, Joffre R, Rambal S. 2011. Is selective thinning an adequate practice for adapting *Quercus ilex* coppices to climate change? *Annals of Forest Science* **68**: 575–585.

Rossi S, Anfodillo T, Čufar K, Cuny HE, Deslauriers A, Fonti P, Frank D, Gričar J, Gruber A, King GM *et al.* 2013. A meta-analysis of cambium phenology and growth: linear and non-linear patterns in conifers of the northern hemisphere. *Annals of Botany* **112**: 1911–1920.

Rossi S, Deslauriers A, Anfodillo T, Carraro V. 2007. Evidence of threshold temperatures for xylogenesis in conifers at high altitudes. *Oecologia* **152**: 1–12.

Rossi S, Deslauriers A, Anfodillo T, Morin H, Saracino A, Motta R, Borghetti M. 2006. Conifers in cold environments synchronize maximum growth rate of tree-ring formation with day length. *New Phytologist* **170**: 301–310.

Rossi S, Deslauriers A, Griçar J, Seo JW, Rathgeber CB, Anfodillo T, Morin H, Levanic T, Oven P, Jalkanen R. 2008. Critical temperatures for xylogenesis in conifers of cold climates. *Global Ecology and Biogeography* **17**: 696–707.

Rossi S, Girard M-J, Morin H. 2014. Lengthening of the duration of xylogenesis engenders disproportionate increases in xylem production. *Global Change Biology* **20**: 2261–2271.

Rossi S, Morin H, Deslauriers A, Plourde PY. 2011. Predicting xylem phenology in black spruce under climate warming. *Global Change Biology* **17**: 614–625.

Ruffault J, Martin-StPaul N, Duffet C, Goge F, Mouillot F. 2014. Projecting future drought in Mediterranean forests: bias correction of climate models matters!. *Theoretical and Applied Climatology* **117**: 113–122.

Ruffault J, Martin-StPaul NK, Rambal S, Mouillot F. 2013. Differential regional responses in drought length, intensity and timing to recent climate changes in a Mediterranean forested ecosystem. *Climatic Change* **117**: 103–117.

Saxton K, Rawls WJ, Romberger J, Papendick R. 1986. Estimating generalized soil-water characteristics from texture. *Soil Science Society of America Journal* **50**: 1031–1036.

Steppe K, De Pauw DJ, Lemeur R, Vanrolleghem PA. 2006. A mathematical model linking tree sap flow dynamics to daily stem diameter fluctuations and radial stem growth. *Tree Physiology* **26**: 257–273.

Subedi N, Sharma M. 2013. Climate–diameter growth relationships of black spruce and jack pine trees in boreal Ontario, Canada. *Global Change Biology* **19**: 505–516.

Swidrak I, Gruber A, Kofler W, Oberhuber W. 2011. Effects of environmental conditions on onset of xylem growth in *Pinus sylvestris* under drought. *Tree Physiology* **31**: 483–493.

Woodruff DR, Meinzer FC. 2011. Water stress, shoot growth and storage of non-structural carbohydrates along a tree height gradient in a tall conifer. *Plant, Cell & Environment* **34**: 1920–1930.

Zweifel R, Eugster W, Etzold S, Dobbertin M, Buchmann N, Hasler R. 2010. Link between continuous stem radius changes and net ecosystem productivity of a subalpine Norway spruce forest in the Swiss Alps. *New Phytologist* **187**: 819–830.

Zweifel R, Zimmermann L, Zeugin F, Newbery DM. 2006. Intra-annual radial growth and water relations of trees: implications towards a growth mechanism. *Journal of Experimental Botany* **57**: 1445–1459.

Supporting Information

Additional supporting information may be found in the online version of this article.

Fig. S1 Metrics used to assess the threshold water potential for growth interruption threshold of plant water potential.

Fig. S2 Relationship between the spring onset of growth and the January–March temperature.

Fig. S3 Relationships between carbon fluxes, annual growth and water deficit.

Table S1 A summary of different methods tested to compute the onset of BA increment

Table S2 Correlations between basal growth, net ecosystem photosynthesis, length of growth periods and critical dates of the growth pattern

Table S3 Pearson correlation coefficient (r) P-value for the correlation between the growth stages and climatic variables considered at the yearly, seasonal and monthly timescales, for the 2004–2011 period

Table S4 Yearly and seasonal climate features derived from the outputs of the regional climate model ALADIN for three periods under the A1B scenario of the IPCC 2007

Methods S1 Site description.

Methods S2 Methods of determination of the t_0.

Methods S3 Identification of the plant water potential for summer growth interruption.

Methods S4 Ecosystem carbon flux measurements.

Methods S5 Statistical analysis.

Please note: Wiley Blackwell are not responsible for the content or functionality of any supporting information supplied by the authors. Any queries (other than missing material) should be directed to the *New Phytologist* Central Office.